

Spin transport in the bulk of two-dimensional Hall insulator

Cite as: Appl. Phys. Lett. **114**, 062403 (2019); <https://doi.org/10.1063/1.5078730>

Submitted: 28 October 2018 . Accepted: 28 January 2019 . Published Online: 13 February 2019

L. V. Kulik , A. V. Gorbunov , A. S. Zhuravlev , V. A. Kuznetsov , and I. V. Kukushkin



View Online



Export Citation



CrossMark

ARTICLES YOU MAY BE INTERESTED IN

[Room temperature multiferroicity and magnetoelectric coupling in Na-deficient sodium bismuth titanate](#)

Applied Physics Letters **114**, 062902 (2019); <https://doi.org/10.1063/1.5078575>

[Comparing the anomalous Hall effect and the magneto-optical Kerr effect through antiferromagnetic phase transitions in \$\text{Mn}_3\text{Sn}\$](#)

Applied Physics Letters **114**, 032401 (2019); <https://doi.org/10.1063/1.5066557>

[Direct observation of the reciprocity between spin current and phonon interconversion](#)

Applied Physics Letters **114**, 052402 (2019); <https://doi.org/10.1063/1.5083207>



Measure Ready
M91 FastHall™ Controller

A revolutionary new instrument
for complete Hall analysis

 Lake Shore
CRYOTRONICS

Spin transport in the bulk of two-dimensional Hall insulator

Cite as: Appl. Phys. Lett. **114**, 062403 (2019); doi: [10.1063/1.5078730](https://doi.org/10.1063/1.5078730)

Submitted: 28 October 2018 · Accepted: 28 January 2019 ·

Published Online: 13 February 2019



View Online



Export Citation



CrossMark

L. V. Kulik,¹  A. V. Gorbunov,¹  A. S. Zhuravlev,¹  V. A. Kuznetsov,^{2,a),b)}  and I. V. Kukushkin^{1,c)}

AFFILIATIONS

¹Institute of Solid State Physics, Russian Academy of Sciences, Chernogolovka 142432, Russia

²National Research University Higher School of Economics, Moscow 101000, Russia

^{a)}Electronic mail: volod_kuzn@issp.ac.ru

^{b)}Also at: Institute of Solid State Physics, Russian Academy of Sciences, Chernogolovka 142432, Russia

^{c)}Also at: National Research University Higher School of Economics, Moscow 101000, Russia

ABSTRACT

Magneto-fermionic condensate under study is a Bose-Einstein condensate of cyclotron spin-flip magnetoexcitons in a quantum Hall insulator. This condensate features unique properties such as millisecond range lifetime and hundreds of micrometers of propagation length. In this study, utilizing the photo-induced resonant reflection technique, we measured the exciton escape time. Finally, we estimated the exciton condensate propagation velocity as 25 m/s, which is much higher than a single particle propagation velocity. We also proposed a mechanism of exciton condensation.

Published under license by AIP Publishing. <https://doi.org/10.1063/1.5078730>

Implementation of new degrees of freedom for solid-state charge carriers creates prospects for developing innovative technological applications. Recent interest has developed in fields of spintronics^{1,2} and magnonics,³ associated with the use of spin waves for information transfer.^{4,5} Interest is growing in the possibility of creating high-temperature Bose-Einstein magnon condensates in yttrium-iron-garnet films, which may facilitate dissipationless transport.^{6,7} New ideas have arisen about signal transfer using exotic collective spin excitations as topological spin structures and skyrmions. Recent research has been reported on the experimental manipulation of separate skyrmions and measurement of their mass and velocity.⁸

Particularly important is the issue of manipulating collective spin excitations in the context of a topological quantum computer utilizing non-Abelian anyons in fractional quantum Hall states (e.g., $5/2$, $12/5$).⁹ This is because nearly all experimentally available information about electron systems in fractional states is provided through conductance of one-dimensional edge channels owing to the bulk being a Hall insulator. Although theory points out a close relationship between the edge and the bulk of Hall insulators, recent experiments on the fractional states $3/2$ and $15/8$ in high-mobility AlGaAs/GaAs heterostructures cast doubt on this relationship.¹⁰ Only the edge of the heterostructures was modified,¹⁰ whereas bulk

states were not affected. Nevertheless, the modification gave rise to Hall resistance plateaus at $3/2$ and $15/8$ resistance quanta. Thus, the correlation between the edge and the bulk is not trivial. Consequently, it is necessary to retrieve additional information from the bulk of Hall insulators. Long-lived spin excitations (magnons analog) are natural candidates for research.

An experiment has recently begun on spin transport in the Hall insulator with the filling factor of $\nu = 2$.^{11,12} The spin carriers are electrically neutral spin cyclotron excitations formed by an electron in the empty first Landau level of the conduction band bound with an electron vacancy (Fermi-hole) in the zero Landau level of the conduction band filled with electrons. Every spin excitation carries spin $S = 1$ and has one of three possible spin projections along the magnetic field axis: $S_z = -1$, 0 , and $+1$ with $S_z = +1$ being the lowest energy excitation.¹³ The spin excitations are optically inactive (dark). Therefore, their lifetime approaches the millisecond range at low temperatures ($T < 1$ K).¹² The long lifetime is not only due to restrictions on direct optical recombination but also due to unusual dispersion: the energy minimum of spin excitations occurs near the reciprocal magnetic length, $q \approx 1/l_B$.¹⁴ The requirement for momentum conservation during the relaxation process extends the excitation lifetime. Due to the long lifetime, it is possible to create a dense ensemble of

spin excitations with integer spin (composite bosons) in a purely fermionic system. Furthermore, single exciton formation time is comparable with the time of luminescence which is about 100 ps.¹¹ As a result, the system undergoes a phase transition to a quasi-equilibrium magneto-fermionic condensate, which produces a sharp increase in the susceptibility to external electromagnetic radiation (super-absorption) and the mean free path for spin excitations.¹² Investigating the magneto-fermionic condensate distribution in the bulk of the Hall insulator provides crucial information about long-range random potential, charge non-uniformity, and artificial obstacles for spin propagation.¹¹ Similar spin excitations are formed near the fractional filling factor of $\nu = 3/2$.¹⁵ The latter fractional quantum-Hall state has been considered a candidate for topological quantum computations.¹⁶

Unfortunately, no direct measurement of the spin dynamics in Hall insulators is possible in experiments on visualization of magneto-fermionic condensate.¹¹ It is unrealistic to form a spin ensemble propagating to macroscopic distances from an excitation spot, which is small compared to the propagation distance, during a single pumping pulse without overheating the electron system. In this paper, we report an experimental study of spin propagation velocity in the bulk of a Hall insulator utilizing the large region of the photoexcitation area. The spin velocity is estimated to be about 25 m/s, which is near the critical superfluid velocity of the magnon condensate (100 m/s) in yttrium-iron-garnet films and significantly exceeds the single magnon propagation velocity.¹⁷ This is an unexpected result. The quantizing magnetic field transforms the two-dimensional electron system into an effectively zero-dimensional system by localizing electrons at the cyclotron orbit scale ($l_B \approx 10$ nm). The spin transport as a correlated motion of the excited electron and the Fermi-hole should, therefore, be separated into a rapid cyclotron precession of two quasi-particles and their slow drift perpendicular to the magnetic field.¹⁸ In reality, we obtain quick lateral motion of the spin excitations through the large pumping spot, which highlights the important coherent transport properties of spin excitations and supplies insight into the physics of bulk states in the Hall insulator.

The experimental studies were performed using a high-quality heterostructure with a symmetrically doped 31 nm GaAs/AlGaAs quantum well. The electron concentration in the two-dimensional channel was $1.9 \times 10^{11} \text{ cm}^{-2}$ and dark mobility exceeded $1.5 \times 10^7 \text{ cm}^2/\text{V} \cdot \text{s}$. The heterostructure was placed into a cryostat with liquid ^3He , which, in turn, was put into a ^4He cryostat with a superconducting solenoid. Optical measurements were made at $T \approx 0.45 \text{ K}$ with a magnetic field of 3.5 T using the double fiber technique. The $3 \times 3 \text{ mm}$ sample was placed at the distance of 1 mm to the optical fibers with a diameter of $400 \mu\text{m}$ and a numerical aperture of 0.15. Laser diode emission for non-resonant pumping of spin excitations (with the central emission line at 785 nm) was coupled into the first fiber simultaneously with a weak resonant emission from a tunable narrow-band (200 kHz) laser utilized for diagnostics of the spin dynamics. The diameter of the excitation spot was $d_p \approx 1.5 \text{ mm}$. The second fiber was employed to collect the reflected light from the pumping spot and to transfer it onto the entrance slit of a grating spectrometer equipped with a cooled CCD camera.

Alternatively, the reflected light was transmitted through a narrow-band interference filter (FWHM = 1.1 nm) and directed to a silicon avalanche photodiode to study the kinetics of resonance reflection. A pair of crossed linear wire-grid polarizers, fixed between the ends of the fibers and the sample, was used to block the strong background signal due to the non-resonant light reflection/scattering at the sample surface and at the ends of the fibers. Circularly polarized light is absorbed and emitted by electrons in a magnetic field. Therefore, the resonant reflection signal from the electron system passes through the linear polarizer that is placed in front of the collecting fiber (Fig. 2). As the linearly polarized light after the non-resonant reflection/scattering remains unchanged, this signal is suppressed by the crossed polarizer.

The dynamics of non-equilibrium spin excitations was explored using a rectangular pulse generator with rise/fall times $< 10 \text{ ns}$. To record the resonance reflection signal, an avalanche photodiode and a gated photon counter were used (Fig. 2). By varying the pumping pulse parameters, such as pulse duration τ_p , repetition period Δt , and peak power density, we characterized both the gas phase of spin excitations and the magneto-fermionic condensate. The gas phase excitations cannot leave the pumping spot because of the short mean free path of a single excitation.¹¹ By comparison, the magneto-fermionic condensate leaves the pumping spot once formed. The decay time of the resonance reflection signal (τ_d) after the pumping pulse is the time for spin excitations to either relax to the ground state or to leave the pumping spot. When the relaxation time is much less than the time to leave the pumping spot, the resonant reflection signal measures the dynamics of spin relaxation to

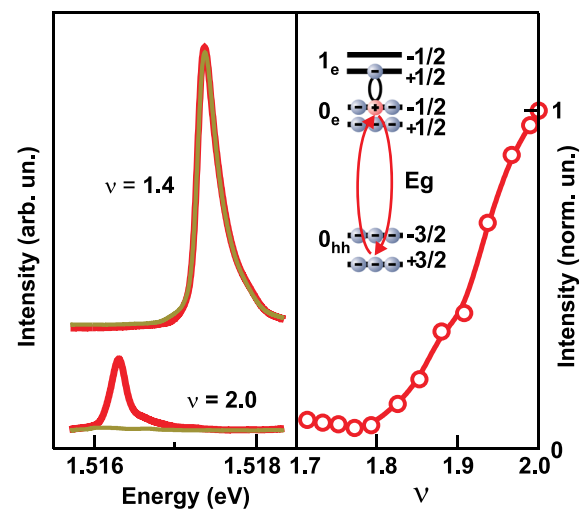


FIG. 1. At left, resonant reflection spectra in the Hall conductor $\nu = 1.4$ and the Hall insulator $\nu = 2.0$ with (red lines) and without (green lines) nonequilibrium spin excitations. At right, the filling factor dependence of the integral differential resonant reflection signal (the difference of reflection signals with pumping “on” and “off”). In the inset, a representation of the optical transitions for resonant reflection with the pumping “on” (0_e and 1_e designate the zero and the first electron Landau level, and 0_{hh} designates the zero Landau level for heavy holes in the valence band of the AlGaAs/GaAs quantum well).

the ground state. In the opposite limit, it measures the dynamics of spin propagation out of the pumping spot. The velocity that the spin excitations acquire leaving the pumping spot can be estimated as $v_c \approx d_p/2\tau_d$. The pulse repetition period Δt should be large enough for spin excitations escaping from the pumping spot to relax to the ground state before the next pumping pulse. In our experiment, the pulse repetition period Δt was chosen to be 10 ms, which is far above any characteristic time of the resonant reflection kinetics.

Figure 1 shows the resonant reflection spectra associated with the empty electron states in the zero Landau level at filling factors $\nu = 1.4$ and 2.0 (Hall insulator). Without optical pumping, no resonant reflection signal is observed at $\nu = 2.0$. It is a trivial result because the absorption and re-emission of resonant light are impossible without vacancies in the zero electron Landau level. As the filling factor is reduced to 1.4 , a resonant reflection appears from the states in the upper spin sublevel of the zero electron Landau level. In this case, switching the laser diode on and off has no effect; the resonant reflection signal remains unchanged. On the other hand, there is a resonant reflection signal for the Hall insulator upon turning the laser diode on. This generates a significant number of non-equilibrium Fermi-holes

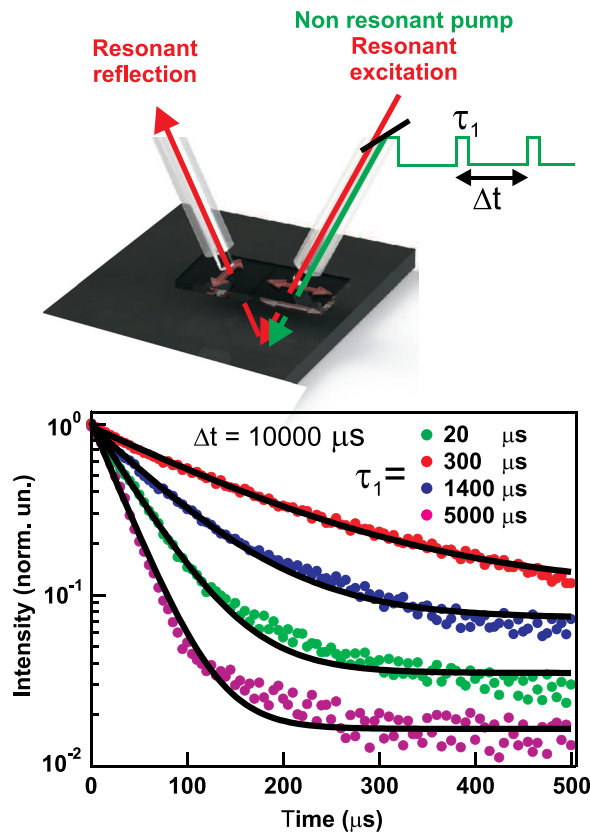


FIG. 2. At top, diagram of the experimental setup. At bottom, the kinetics of resonant reflection signal decay after the end of the pumping pulse at different pumping pulse durations τ_p measured in the Hall insulator at $\nu = 2.0$. Solid curves are results of fitting with an exponential function.

at the upper spin sublevel of the zero electron Landau level. The ratio of the reflection signal intensity at $\nu = 1.4$ and $\nu = 2.0$ provides an estimate of the pumped non-equilibrium spin density.

Examples of Photo-induced Resonant Reflection (PRR) kinetics in the Hall insulator at $\nu = 2.0$ measured at different pumping pulse widths τ_p and a fixed repetition period Δt are presented in Fig. 2. Three characteristic regions can be distinguished by the dependence of the reflection signal decay time on the pump pulse width $\tau_d(\tau_p)$ (Fig. 3). Region 1 is related to the low non-equilibrium spin density (of order 0.01 of the number of electron states in a single spin Landau sublevel¹⁸). Here, spin excitations primarily occupy states with zero momentum, $q = 0$. In Region 2, spin excitations start to occupy states near the minima of the dispersion curve, $q \approx 1/l_B$.¹⁹ Whereas in Region 1, filling of these states is hindered because of conservation of momentum requirements ($1/l_B \approx 10^6 \text{ cm}^{-1}$); Region 2 fills these states due to two-particle scattering mechanisms. Relaxation to the ground state is then inhibited because the relaxation mechanisms involve energy transfer and a large momentum transfer.

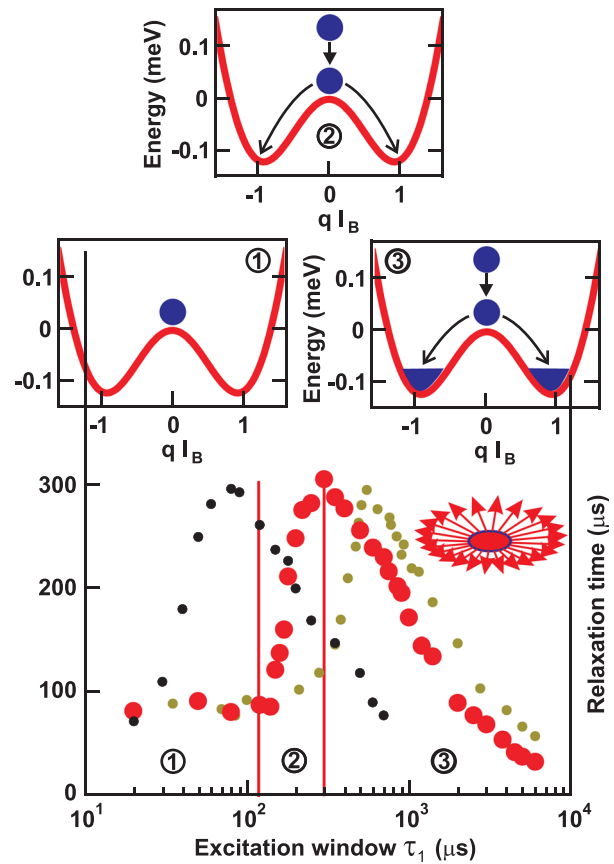


FIG. 3. The decay time τ_d of the resonant reflection signal as a function of the pumping pulse duration τ_p measured at the peak pump power of $50 \mu W$ (large red dots). For comparison, similar dependencies are shown for $100 \mu W$ (black dots) and $25 \mu W$ (grey dots). At top, three subsequent states of non-equilibrium ensemble of spin excitations (Regions 1, 2, and 3) are shown. In the inset, an illustration of lateral spin transport from the pumping spot.

Finally, Region 3 displays the escape of spin excitations from the excitation spot.¹¹ The total relaxation rate (sum of the relaxation rate to the ground state and the rate of escape from the pumping spot) then increases (Fig. 3). The majority contribution is the fraction of spin excitations that escape from the pumping spot. Figure 3 shows that at the end of Region 3, the time for spin excitations to escape from the pumping spot is about 10 times shorter than the time for spin excitations to relax to the ground state. Therefore, we can disregard the contribution of the relaxation to the ground state in the total measured decay time of 30 μ S. Thus, the average velocity that spin excitations acquire in the magneto-fermionic condensate before crossing the edge of the excitation spot is about 25 m/s. Due to such rapid spin propagation, the spin excitations become very promising candidates for signal transfer in Hall insulators.

This work was supported by the Russian Science Foundation Grant No. 18-72-00126.

REFERENCES

- ¹M. N. Baibich, J. M. Broto, A. Fert, F. N. Van Dau, F. Petroff, P. Etienne, G. Creuzet, A. Friederich, and J. Chazelas, *Phys. Rev. Lett.* **61**, 2472 (1988).
- ²G. Binasch, P. Grünberg, F. Saurenbach, and W. Zinn, *Phys. Rev. B* **39**, 4828 (1989).
- ³V. V. Kruglyak, S. O. Demokritov, and D. Grundler, *J. Phys. D: Appl. Phys.* **43**, 264001 (2010).
- ⁴A. V. Chumak, V. I. Vasyuchka, A. A. Serga, and B. Hillebrands, *Nat. Phys.* **11**, 453 (2015).
- ⁵Y. Kajiwar, K. Harii, S. Takahashi, J. Ohe, K. Uchida, M. Mizuguchi, H. Umezawa, H. Kawai, K. Ando, K. Takanashi, S. Maekawa, and E. Saitoh, *Nature* **464**, 262 (2010).
- ⁶S. O. Demokritov, V. E. Demidov, O. Dzyapko, G. A. Melkov, A. A. Serga, B. Hillebrands, and A. N. Slavin, *Nature* **443**, 430 (2006).
- ⁷V. E. Demidov, S. Urazhdin, B. Divinskiy, V. D. Bessonov, A. B. Rinkevich, V. V. Ustinov, and S. O. Demokritov, *Nat. Commun.* **8**, 1579 (2017).
- ⁸F. Büttner, C. Moutafis, M. Schneider, B. Krüger, C. M. Günther, J. Geilhufe, C. V. Korff Schmising, J. Mohanty, B. Pfau, S. Schaffert, A. Bisig, M. Foerster, T. Schulz, C. A. F. Vaz, J. H. Franken, H. J. M. Swagten, M. Kläui, and S. Eisebitt, *Nat. Phys.* **11**, 225 (2015).
- ⁹C. Nayak, S. H. Simon, A. Stern, M. Freedman, and S. D. Sarma, *Rev. Mod. Phys.* **80**, 1083 (2008).
- ¹⁰H. Fu, P. Shan, P. Wang, Z. Zhu, L. N. Pfeiffer, K. W. West, and X. Lin, e-print [arXiv:1702.02403v1](https://arxiv.org/abs/1702.02403v1).
- ¹¹L. V. Kulik, V. A. Kuznetsov, A. S. Zhuravlev, A. V. Gorbunov, V. V. Solov'yev, V. B. Timofeev, I. V. Kukushkin, and S. Schmult, *Sci. Rep.* **8**, 10948 (2018).
- ¹²L. Kulik, A. Zhuravlev, S. Dickmann, A. Gorbunov, V. Timofeev, I. Kukushkin, and S. Schmult, *Nat. Comm.* **7**, 13499 (2016).
- ¹³L. V. Kulik, I. V. Kukushin, S. Dickmann, V. E. Kirpichev, A. B. Van'kov, A. L. Parakhonsky, J. H. Smet, K. V. Klitzing, and W. Wegscheider, *Phys. Rev. B* **72**, 073304(4) (2005).
- ¹⁴C. Kallin and B. I. Halperin, *Phys. Rev. B* **30**, 5655–5614 (1984).
- ¹⁵A. S. Zhuravlev, L. V. Kulik, V. A. Kuznetsov, M. A. Khitko, and I. V. Kukushkin, *JETP Lett.* **108**, 419 (2018).
- ¹⁶J. Falson, D. Maryenko, B. Friess, D. Zhang, Y. Kozuka, A. Tsukazaki, J. H. Smet, and M. Kawasaki, *Nat. Phys.* **11**, 347 (2015).
- ¹⁷C. Sun, T. Nattermann, and V. L. Pokrovsky, *J. Phys. D: Appl. Phys.* **50**, 143002 (2017).
- ¹⁸Y. Qi and S. Zhang, *Phys. Rev. B* **67**, 052407 (2003).
- ¹⁹V. A. Kuznetsov, L. V. Kulik, M. D. Velikanov, A. S. Zhuravlev, A. V. Gorbunov, S. Schmult, and I. V. Kukushkin, *Phys. Rev. B* **98**, 205303 (2018).